Available online at www.sciencedirect.com
ScienceDirect
Journal of Power Sources 165 (2007) 65–72
JOURNAL OF POWER SOURCES
www.elsevier.com/locate/jpowsour

Platinum-plated nanoporous gold: An efficient, low Pt loading electrocatalyst for PEM fuel cells

Roswitha Zeis, Anant Mathur, Greg Fritz, Joe Lee, Jonah Erlebacher*

Department of Materials Science and Engineering, Johns Hopkins University, Baltimore, MD 21218, United States

Received 15 November 2006; received in revised form 1 December 2006; accepted 5 December 2006
Available online 16 January 2007

Abstract

Platinum-plated nanoporous gold leaf (Pt-NPGL) is made by coating a conformal, atomically thin skin of platinum over the high surface area pores of a thin membrane of nanoporous gold. Because Pt loading in Pt-NPGL can be controlled down to 0.01 mg cm^{-2} using only simple benchtop chemistry, the material holds promise as a low Pt loading, carbon-free electrocatalyst. Here, we report successful use of Pt-NPGL as a catalyst in proton exchange membrane (PEM) fuel cells. Stable and high performance Pt-NPGL/Nafion membrane electrode assemblies (MEAs) were made using a stamping technique. The performance of Pt-NPGL MEAs is comparable to conventional carbon-supported nanoparticles-based MEAs with much higher loading, generating an output power density of up to 4.5 kW g^{-1} Pt in our non-optimized test configuration. Correlations between the performance of Pt-NPGL MEAs, the electrochemically accessible surface area, and material microstructure are discussed. Our success in using Pt-NPGL as a fuel cell catalyst suggests that creating precious metals skins over nanoporous metal supports is a viable strategy for designing new catalysts for PEM fuel cells. This promising approach allows tailoring catalytic activity by engineering precious metal/substrate interactions, employs materials with dual functionality acting both as current collector and catalyst, and may avoid the sintering problems plaguing conventional nanoparticle-based catalysts.

Keywords: Fuel cells; Ultra-low loading Pt catalyst; Nanoporous metals

1. Introduction

The high cost of precious metals used in the conventional proton exchange membrane (PEM) fuel cell, as well as catalyst degredation over long periods of use, poses a tremendous challenge to PEM fuel cell development. Finding new directions to lower cost alternative electrocatalysts is thus critically important for bringing the hydrogen economy closer to reality. Most strategies toward this end currently involve the design of new kinds of nanoparticle catalysts, for instance, made from alloys or intermetallics that use less or no platinum [1–4]. Almost universally, once the nanoparticles are made, they are supported (physisorbed) onto larger carbon particles, and then this composite is further mixed with an ionomer solution which acts as a binder and proton carrier, to form a catalytic ink. However, in the fuel cell environment, catalyst particles tend to agglomerate and sinter over time reducing exposed surface area [5], the carbon support may corrode from beneath them exacerbating this effect [6], and any catalyst particle that loses physical connection to its neighbors becomes electrically disconnected from the external circuit and is rendered useless. Only a few groups are actively pursuing strategies for low load nanoparticle-less Pt catalyst layers. One method employs sputter deposition of ultra-thin films of platinum directly onto roughened Nafion [7]. Although the loading in such cells may be quite small (<0.04 mg cm^{-2}), the current–voltage performance of cells made using this method are still significantly below the performance of state-of-the art nanoparticle-based catalysts.

In our laboratory, we have been experimenting with a new approach to catalyst materials design for PEM fuel cells. In our concept (Fig. 1), a conductive mesoporous metal membrane with pore sizes of order 10 nm acts as a substrate on which an atomically thin layer of catalytic metal, such as Pt is deposited as a "skin" enclosing the porous substrate. If the membrane and the precious metal layer are thin enough (<100 and <1 nm, respectively), then precious metal loads should be controllable

* Corresponding author. Tel.: +1 410 516 6077; fax: +1 410 516 5293.
E-mail address: Jonah.Erlebacher@jhu.edu (J. Erlebacher).

0378-7753/$ – see front matter © 2006 Elsevier B.V. All rights reserved.
doi:10.1016/j.jpowsour.2006.12.007

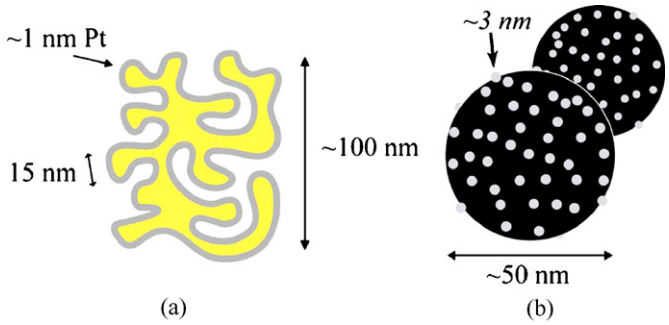

Fig. 1. A new strategy to make high surface area, low-precious metal loading electrocatalysts for PEM fuel cells (a) involves coating the skin of a continuous, conductive and thin (~100 nm) mesoporous membrane substrate (nanoporous gold) with an atomically thin layer of precious metal (platinum). A cartoon with similar scale of conventional supported nanoparticles catalysts (b) highlights the idea that, in contrast to the strategy discussed here, nanoparticles are only weakly physisorbed to carbon supports and may become electrically disconnected from the external circuit if the support erodes or the particles agglomerate. Typical catalyst layers in this configuration are many microns thick.

to less than 0.01 mg cm^{-2}, with nearly every precious metal atom in electrical contact with the external circuit. Furthermore, in this strategy, the support acts both as a catalytic layer and as a current collector, simplifying membrane electrode assembly (MEA) fabrication. More generally, in this substrate/skin approach to catalyst design, new avenues to control catalyst activity can be investigated. For instance, if the skin is epitaxial to the substrate (i.e., extending the crystal structure of the metallic mesoporous substrate into the catalyst layer), there will often be significant lattice strain in the catalyst layer, pushing apart (or pushing together) the catalyst atoms relative to their spacing in nanoparticle form. For reactions that are sensitive to the catalyst lattice parameter, such as CO adsorption and subsequent poisoning [8], such control over the lattice parameter may lead to new materials that are resistant to CO poisoning.

Here, we report success in bringing our concept of mesoporous metal substrate/skin electrocatalyst design to reality by integrating platinum-plated nanoporous gold leaf (Pt-NPGL) membranes into Nafion-based MEAs, and testing the performance of these MEAs in conventional H_2/O_2 PEM fuel cells. Pt-NPGL is made by starting with a thin sheet of silver/gold [9,10]. We use sheets in the form of "leaf", a material traditionally used by artists for decoration, but with attributes particularly convenient for our purposes. Leaf is a mechanically hammered foil, only ~100 nm thick that is made in a batch processing technique which produces thousands of sheets simultaneously with no material waste. Typical dimensions of commercially available leaf are 3(3/8)in. × 3(3/8)in. or ~70 cm^2, but could be arbitrarily larger if required. We use leaf with a 50/50 composition by weight ($Ag_{65}Au_{35}$), because at this composition the material may be dealloyed of silver by floating the leaf in a bath of nitric acid to produce a free-standing membrane of nanoporous gold which possesses open porosity and typical pore size ~15 nm. Pictures and micrographs of the material may be found in Ref. [10]; an SEM micrograph of nanoporous gold is shown in Fig. 2a. At this point, the thickness of the nanoporous gold membrane varies between 100 and 130 nm, usually nearer to 100 nm, as evidenced by cross-sectional scanning electron microscopy (SEM). The void fraction is ~60%, consistent with weight measurements that give the total gold loading at 0.11–0.12 mg cm^{-2}. The membrane is highly conductive. Ideally, we would like to replace nanoporous gold with a less expensive substrate material, such as silver, but to date no one has discovered a way to create a nanoporous silver membrane. As it is, commercial prices for gold leaf are about US$ 6 m^{-2} as of the time of writing.

Conformal skins of platinum can be plated upon nanoporous gold leaf using a variation of electroless deposition in which the leaf is placed at the interface between a bath containing a platinum salt solution, and a vapor containing a reducing agent. In earlier work [11], we showed that reduction of Pt is confined to the pores of the leaf; furthermore, as the pores get filled locally, reactant mass transport is reduced in that region, allowing other regions to catch up. An SEM micrograph of Pt-plated nanoporous gold leaf (Pt-NPGL) is shown in Fig. 2b. In the end, the technique gives a high degree of control over the Pt-plating rate. Loading can be controlled to within 0.01 mg cm^{-2}, or approximately one atomic monolayer of platinum covering the substrate. Interestingly, as we discuss in detail below, the Pt layer is epitaxial to the nanoporous gold substrate, so that the NPG crystal lattice is extended into the catalytic overlayer. Thus, Pt is not in the form of adsorbed nanoparticles; rather, it is strongly bound to the substrate and in intimate electrical contact with it. This attribute may help the long-term stability of Pt-NPGL, and also suggests that Pt-NPGL can double as catalyst and current collector. Additionally, the fact that we can control the Pt loading to a high degree has allowed us to conduct a study of MEA performance with varying Pt loading, from which we have been able to identify optimal points.

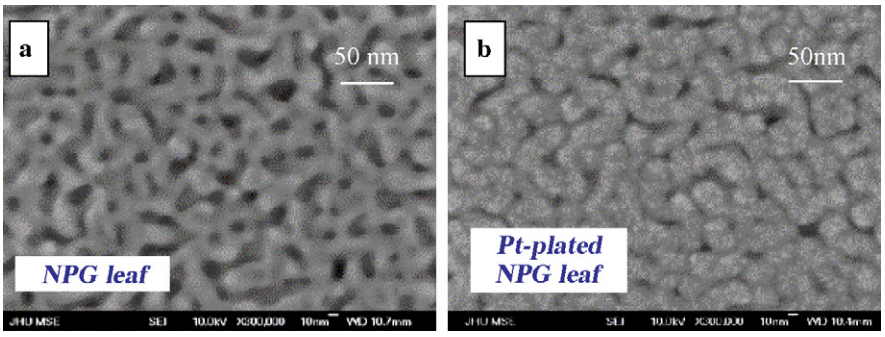

Fig. 2. SEM micrographs of (a) dealloyed nanoporous gold leaf and (b) Pt-plated nanoporous gold leaf ("high" loading of ~0.05 mg cm^{-2}).

We believe that integration of Pt-NPGL into actual, stable, Nafion-based MEAs is the most viable method to demonstrate the utility of this (or any) new catalyst material for fuel cell technologies, and this is the primary subject of the work here. Strictly from a performance standpoint, our Pt-NPGL fuel cells generate upwards of 240 mW cm^{-2} with Pt loadings less than 0.05 mg cm^{-2} using the material both as anode and cathode catalyst. To date, our best cells achieve an output power density of up to 4.5 kW g^{-1} Pt. Catalyst layers with electrochemically active surface areas greater than 50 m^2 g^{-1} Pt are easily fabricated using simple benchtop chemistry at room temperature. In our cell geometry, Pt-NPGL acts both as a current collector and catalyst, and thus the entire MEA is virtually no thicker than the Nafion membrane on which the catalytic electrodes are supported. These characteristics suggest that Pt-NPGL may be particularly useful where thin form factors are important (such as micro-fuel cells), but the performance in our unoptimized test apparatus suggests that there is still room to greatly enhance Pt-NPGL performance and its ultimate applicability.

2. Experimental

2.1. Preparation of the Pt-NPGL electrocatalyst

The preparation of Pt-NPGL has been reported in Ref. [11]. Briefly, the substrate backbone of the electrode is an approximately 100-nm thick free-standing thin film of nanoporous gold leaf (NPGL), which was prepared by dealloying 12-carat white gold leaf ("Monarch" brand, Sepp Leaf Products Inc., NY) by floating it upon a bath of concentrated nitric acid for 5 min. This process resulted in a conductive sheet of nanoporous gold with a pore size around 15 nm. In leaf form, the gold content of NPGL is typically ~0.12 mg cm^{-2}; slight variations both upward and downward are found. The material possesses a high specific surface area on the order of 10 m^2 g^{-1} and a high in-plane conductivity. Being gold, it is chemically inert. The use of gold in a fuel cell might at first glance be troubling as gold is known to catalyze peroxide formation from oxygen and hydrogen which can degrade organics within the cell [12,13]. However, as we will show, plating this substrate with Pt effectively hides it from the reactant gas flow, and we see no evidence of peroxide formation. Furthermore, because there is no carbon support for the catalyst, degredation of the catalyst via peroxide seems an unlikely possibility.

Platinum-plating of NPGL membranes was made by a variation of standard electroless plating methods [11]. Briefly, one floats a piece of nanoporous gold leaf on a solution containing Pt ions in suspension (2 mM $Na_2Pt(OH)_6$ salt buffered to a pH value of 9.9 using NaOH) and then one flows a vapor of the reducing agent hydrazine over the leaf, i.e., the leaf membrane is at the interface between the metal ions and the reducing agent. By separating the platinum ions and the reducing agent in this way, the plating reaction is confined to within the pores, self-limiting, and results in a conformal and uniform coating of Pt over the NPGL substrate, including over the surfaces of the interior pores. The plating reaction kinetically shuts down before the Pt layer reaches even 5 nm, so the pores stay open, a necessary feature to ultimately allow reactant gas flow in the cell. The Pt loading typically reached a maximum of approximately 0.05 mg cm^{-2} as determined by precise weight measurements of large area (50 cm^2) samples before and after platinum deposition.

2.2. Preparation of membrane electrode assemblies

To prepare Pt-NPGL MEAs, Pt-NPGL membranes were floated on a water bath and lifted from below onto mica disks with a diameter of 2.2 cm (geometric area of 3.8 cm^2) and a thickness of about 150 μm. Fig. 3a shows a photo of Pt-NPGL membranes floating on water and then dried onto mica disks after catching them from below. Up to nine mica disks could be coated with porous gold in one batch. Nafion 113.5 was used as the proton exchange membrane. Nafion was cleaned and activated using

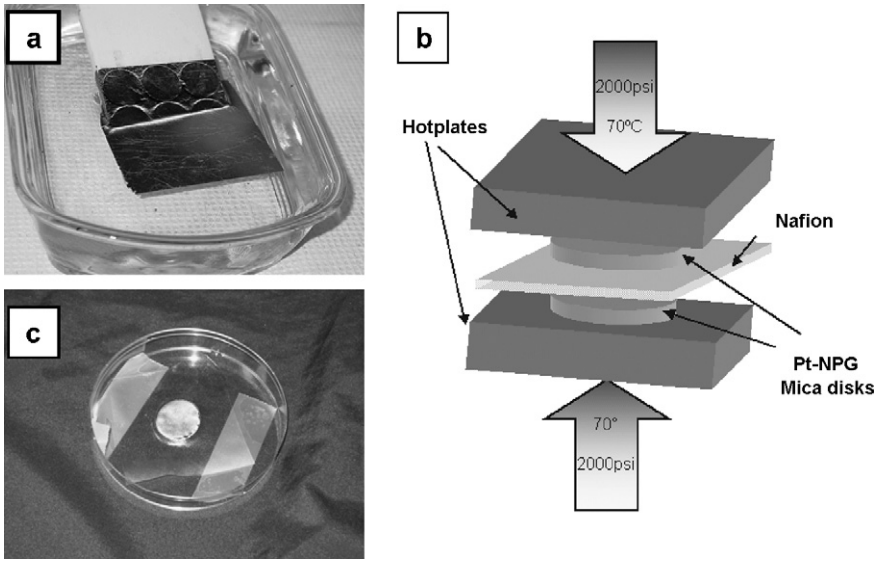

Fig. 3. MEA fabrication. (a) A sample of Pt-NPGL is floated upon a water bath, mica sheets catch them from below, and then they are dried, (b) the stamping procedure used to produce the MEA and (c) final MEA. The active area has a diameter of 2.2 cm.

the standard methods of boiling in 5% peroxide solution, followed by submersion in a bath of concentrated sulfuric acid. The Pt-NPGL membranes were transferred to the Nafion 113.5 surfaces by a stamping technique shown in Fig. 3b. Here, the mica disks served as stamps to "print" the porous gold leaf onto both sides of the Nafion simultaneously. During the stamping process, a moisturized Nafion membrane was sandwiched between two mica disks with their Pt-NPGL coated surfaces facing the Nafion. The assembly was then hot pressed at a temperature of about 70 °C and a pressure of about 2000 psi for approximately 5 min. During pressing, the Pt-NPGL membranes lifted off the mica and became firmly bonded to Nafion, and the mica disks easily detached from the MEA. A photograph of a "hot-pressed" Pt-NPGL MEA is shown in Fig. 3c.

The attachment of Pt-NPGL to moisturized Nafion at intermediate temperatures is central to the viability of the cells. Much of the irreproducibility of the prototype cell we reported in Ref. [11], we now hypothesize, can be ascribed to tearing of the fragile mesoporous metal by overmoisturizing and swelling of Nafion, or to degredation of the MEA when treated at temperatures greater than 100 °C, which we had done to improve adhesion prior to our use of hot-pressing.

2.3. Characterization of fuel cell performance using Pt-NPGL MEAs

As-prepared Pt-NPGL MEAs were tested and characterized in the fuel cell environment by first sandwiching them between two pieces of Teflon treated carbon cloth (EC-CC1-060T, ElectroChem, Inc.), then in turn sandwiching the MEA/carbon cloth between two stainless steel current collection plates on which serpentine gas flow channels had been machined into an area of 10 cm^2. The entire structure was gasketed using silicone gasketing material. Hydrogen and oxygen were humidified using bubble humidifiers and fed into the fuel cell through heated gas lines. Typical operating pressures and gas flow rates were 50 psi, 1–10 sccm, respectively, although these values were generally adjusted slightly up or down "on the fly" to stabilize and enhance performance. Cell performance was assessed through voltage–current (*VI*) performance and through measurement of the electrochemically active surface area (ECA) using a standard measurement in which a potentiostat is configured with the anode as working and reference electrode, and the cathode as counter electrode [14]. A commercial MEA (FuelCell store item #597010, 4 cm^2 area, Nafion 112, 0.5 mg Pt cm^{-2} cathode and anode loading) was used for comparison and run under the same conditions as the Pt-NPGL MEAs.

Pt-NPGL MEAs with identical cathode and anode loadings from 0.01 to 0.05 mg cm^{-2} were fabricated for testing. The testing cycle we used for each MEA was as follows: first, the MEA was heated to at 75 °C and operated using H_2/O_2 for several hours to ensure that the Nafion membrane was sufficiently moisturized and impurities are washed out of the cell system. Then, the cell was cooled to room temperature, the oxygen flow was replaced by nitrogen, and the MEA was subjected to ten potential cycles in the ECA configuration, ramping the potential between cathode and anode between 0.03 and 1.5 V at a sweep rate of 550 mV s^{-1}. These cycles tended to activate and perhaps purify the electroactive Pt surface possibly by oxidizing and removing impurities adsorbed on the surface of the electrode during sample preparation. We found that subjecting samples to this preliminary cyclic voltammetry (CV) increased the electroactive surface area, and cell performance became much more reproducible.

After the pre-cleaning step, the electrochemically active surface area of the membrane electrodes was found by integrating hydrogen adsorbtion on the cathode electrode [14]. Cyclic voltammograms (CV) for ECA determination were measured using a Gamry Z750 potentiostat. During the ECA measurements, the cell was held at room temperature (22 °C) and the cathode was purged with nitrogen. ECA values were calculated from the integrated charge found from hydrogen adsorption and desorption cyclic voltammograms, corrected for shorting and hydrogen crossover, and assuming 210 μC cm^{-2} of Pt surface area at saturation coverage. CVs were obtained with a scan rate of 550 mV s^{-1}. After the ECA of the membrane was found, the nitrogen flow was replaced by oxygen, the cell was heated to 75 °C, and voltage–current data was collected using an electronic load (Array 3710A).

3. Results and discussion

3.1. The microstructure of Pt-NPGL versus load

The loading versus plating time and its correlation to the microstructure of Pt-NPGL is illustrated in Figs. 4 and 5. Fig. 5 shows the load versus plating time (exposure to hydrazine vapor), and illustrates that the loading can be easily controlled from 0.01 to 0.05 mg cm^{-2}. The surface area of the pores of NPGL has been found to be ~10 cm^2 cm^{-2} of geometric area. Using the density of Pt, we can roughly estimate the

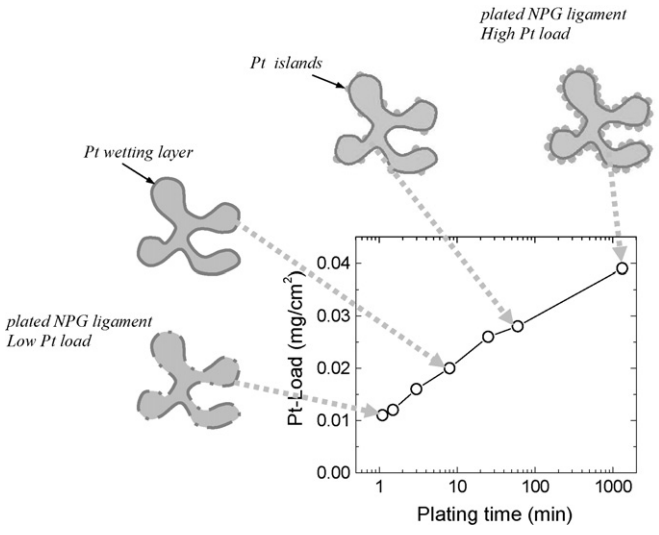

Fig. 4. (Graph) Pt load vs. plating time (a–d) cartoons of the evolution of the platinum on porous gold microstructure. At early times, a uniform, thin wetting layer is deposited. As the platinum load increases, the strain energy in the deposited layer becomes large enough that the surface becomes islanded. Micrographs corresponding to the cartoons (a–d) are found in Fig. 5.

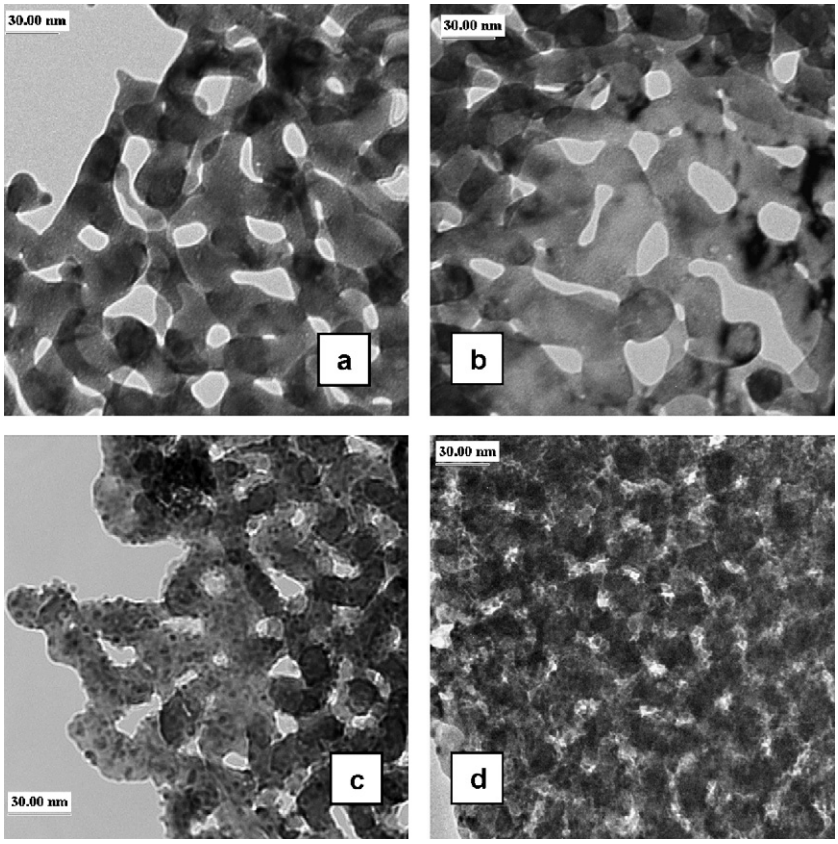

Fig. 5. Transmission electron micrographs of Pt-NPGL membranes corresponding to points on the Pt loading curve of Fig. 4.

Pt loading to correspond to ∼2 monolayers (ML) at the low end (0.01 mg cm^{-2}) increasing to ∼10 ML at the high end (0.05 mg cm^{-2}). Transmission electron microscopy of samples with differing amounts of Pt-plating correlated to the load measurement are shown in Fig. 6. It is only when 5–6 ML of Pt (∼2 nm) are deposited that the surface undergoes a morphological transition and becomes bumpy.

Based on our observations, we believe that the growth of Pt on NPGL can be described as the Stranski–Krastanov mode [11,15], a strained layer epitaxial crystal growth mode in which a smaller lattice parameter material is deposited onto a substrate with a larger lattice parameter. Here, Pt has a 4% smaller lattice parameter than Au, and we also know from previous work that deposition is epitaxial [11,16]. In the initial stages of growth, the lattice mismatch is accommodated by an elastic strain of the Pt layer; in fact, one would expect the lattice parameter of Pt at this stage to be that of gold. Thus, in the early stages (<0.028 mg cm^{-2}), Pt forms a "wetting layer" uniformly coating the NPG substrate. However, Pt strain energy increases sharply with continued growth, and after a few monolayers Pt growth switches to a lower energy mode via formation of partially strain-relaxed three-dimensional islands. Islands are energetically favorable because they can relieve their in-plane strain by relaxing out-of-plane. These epitaxial islands of Pt are uniform in size and are evenly distributed over the substrate. Thus, in the late stages of growth we might expect that the surface area is slightly increased relative to that in the low Pt load samples, and that the lattice parameter of surface Pt is closer to that of bulk Pt; of course, in the late stages, there is also buried Pt, so the overall Pt load will be higher.

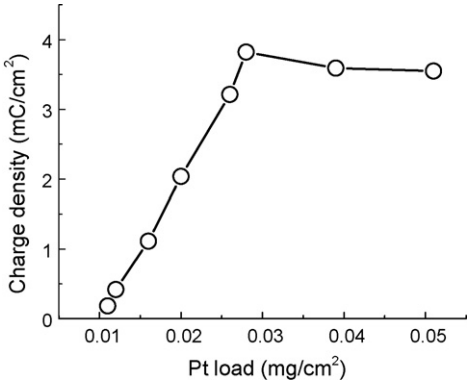

Fig. 6. Charge density corresponding to adsorbed hydrogen on Pt-NPGL MEAs vs. Pt load.

An important aspect to consider regarding the growth is the potential formation of surface alloys in the early stages of growth. We cannot discount this possibility, however, the Au–Pt (bulk) phase diagram shows only limited solubility at room temperature, where we have done all our processing. Studies of vacuum-deposited epitaxial Pt on Au(l l 1) have shown that there is substantial intermixing during the first monolayer of deposition, but the second monolayer deposited is pure Pt [17]. In our case, any intermixing cannot be more than just a couple of atomic layers, because we have also previously shown that one

can completely dissolve away the gold substrate to leave a tenuous nanometer-thick "nanotubular" mesoporous platinum [16]. The lack of extensive intermixing in our system is in contrast to the formation of AuPt alloy nanoparticles by others, but these are usually formed during co-precipitation of gold and platinum, for instance during an electroless reduction [18], a (locally) high deposition rate kinetic process that might lead to the formation of metastable phases.

3.2. Electrochemically active surface area

Eight Pt-NPG MEAs with Pt loads between 0.011 and 0.05 mg cm^{-2} electrode^{-1} were prepared for ECA testing, as well as a commercial MEA, which we used for reference. Typical examples of the hydrogen adsorption/desorption cyclic voltammetry are presented in Fig. 7. The general shapes of the CV curves were similar for all Pt-NPGL MEAs (Fig. 7b and c) and the commercial MEA (Fig. 7a). Hydrogen adsorption/desorption occurs in the potential region between 0.07 and 0.4 V. However, the characteristic double-peak structure representing specific adsorption on the (1 1 0) and (1 0 0) crystallographic faces of a polycrystalline (or at least, polyfaceted) Pt-surface was not present for Pt-NPGL MEA with a low Pt load (<0.028 mg cm^{-2}) as shown in Fig. 7c. Although it has been reported that the detailed structure of this kind of CV could be lost due to impurities on the Pt-surface [19], this is not the likely the explanation for the absence of the double-peak structure in the low Pt load cyclic voltammograms because the double-peak structure is clearly visible in the high Pt load cases (Fig. 7b). We believe the absence of the double-peak structure in the case of low Pt load provides direct evidence that the NPG comprises of (1 1 1)-oriented nanofacets on which Pt has grown an epitaxial thin wetting layer, an observation consistent with our TEM experiments and computer simulations of the structure of nanoporous gold [9]. For the higher Pt loads, the Pt islands that form on top of the wetting layer expose facets other than (1 1 1) and therefore contribute to the polyfaceted character of the cyclic voltammogram. This assumption is further supported by the observation that the net charge density (Fig. 8) associated with the reduction of protons increases linearly with the amount of platinum until it reaches its maximum of 3.8 mC cm^{-2} at a Pt load of 0.028 mg cm^{-2}. This suggests that at the lowest Pt loadings the atomically thin Pt wetting layer is incomplete (or at least less catalytic).

Further increase of the Pt loading beyond 0.028 mg cm^{-2} did not result in a larger net charge density, which remained almost constant as the load increased further. This is likely because the electrode surface had been completely covered with platinum at this load. As a result, adding more Pt makes the wetting layer grow thicker; this increases the Pt load but not the catalytic area.

Fig. 8 shows a summary of the electrochemical surface areas (ECA) plotted as a function of the Pt load. For the commercial MEA, we calculated an ECA of 43 m^2 g^{-1}, a value that is comparable to those reported by others; for our Pt-NPGL MEAs we obtained a maximum ECA of 65 m^2 g^{-1} Pt at a load of 0.028 mg cm^{-2}. These results mean that platinum uniformly coats the nanoporous gold leaf support, a significant amount of the platinum is available for reaction, and that our cells have ECA comparable to commercial MEAs with much higher loading.

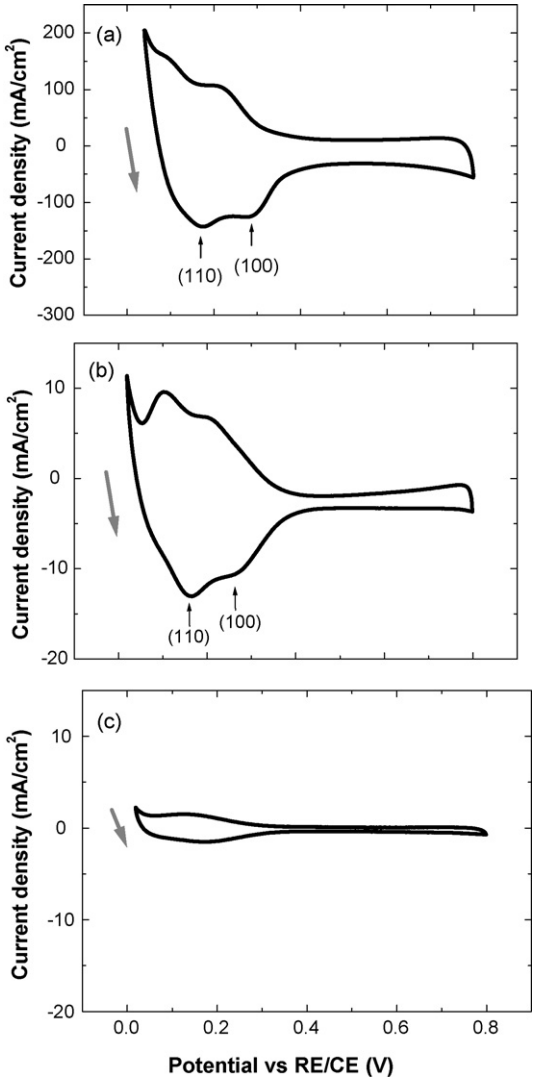

Fig. 7. Cyclic voltammograms for ECA measurements (a) commercial MEA, (b) Pt-NPGL MEA with a Pt load of 0.028 mg cm^{-2} and (c) Pt-NPGL MEA with a Pt load of 0.012 mg cm^{-2}.

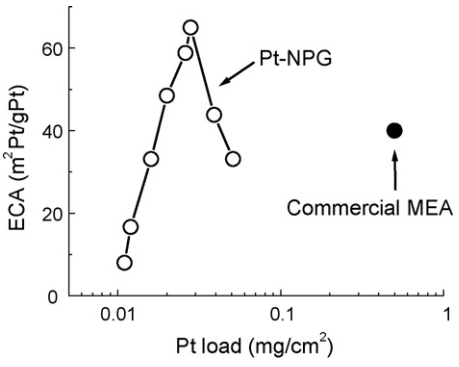

Fig. 8. Electrochemically active surface area (ECA) vs. Pt load (open circles). ECA of a commercial MEA (0.5 mg cm^{-2}) for comparison.

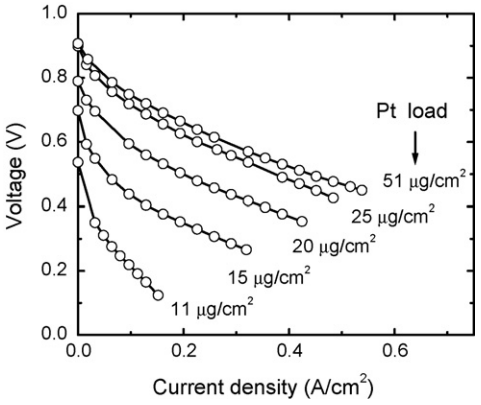

Fig. 9. Voltage–current polarization of Pt-NPGL MEAs with different Pt loads.

3.3. Voltage–current characteristics of Pt-NPGL fuel cells

After completing the hydrogen adsorption experiment, we replaced the nitrogen gas with oxygen, heated the cell to 75 °C and carried out the *VI* measurement. We choose this measurement sequence because the high potential CVs not only improved the ECA, but also the fuel cell performance. Polarization curves of Pt-NPG MEA with different Pt loads are shown in Fig. 9. The open circuit potential varied from 0.55 V for the lowest Pt load to 0.9 V for the higher Pt loads. These open circuit potentials are slightly lower than the open circuit potential of commercial hydrogen/oxygen fuel cells, which is typically about 1 V [20,21]. We think the loss of open circuit potential might be due to the increase of electron conductivity across the Nafion membrane, a result of the stamping process or our procedure for clamping the MEA into the fuel cell test rig, as well as kinetic losses at the cathode using our low loads.

The relation between maximum power density and Pt load is given in Fig. 10. As expected, the cell generates a higher power density with high Pt load. The dependence of power density upon the Pt load is consistent with the charge density measurement presented earlier in Fig. 6. At small loads, the power increases linearly with the amount of Pt, saturating at a maximum of 0.24 W cm^{-2} for a Pt load of 0.028 mg cm^{-2} (at this stage, NPGL is primarily coated with the Pt wetting layer only beginning to become islanded). Similar to the leveling off behavior for the charge density, the initial linear increase is due to the increase of active surface area and the saturation occurs once the entire surface of NPG is covered with Pt.

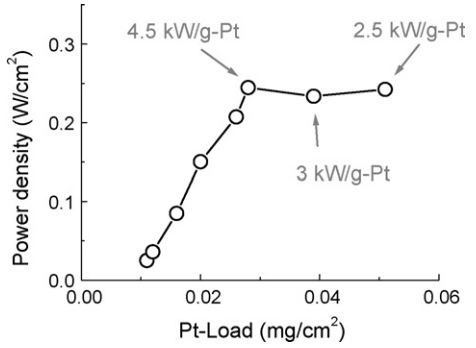

Fig. 10. Maximum power density of Pt-NPGL MEAs vs. Pt load.

The Pt-NPGL fuel cells reported here are able to generate an output power of up to 4.5 kW g^{-1} Pt by at a Pt load of 0.028 mg cm^{-2}, just when the increase in surface area saturates. This is within a factor of two of what is reported for many state-of-the-art fuel cells [20]. Unfortunately, our ultimate power at ultra-low load (∼0.01 mg cm^{-2}) seems limited by a low open circuit potential. Our current speculation is that this problem is related to MEA fabrication and/or our testing apparatus, and we are working to improve these values.

4. Conclusions

We demonstrate that viable alternatives to carbon-supported nanoparticle catalysts may be found in the formation of nanoporous metals with atomically thin catalyst skins, specifically, nanoporous gold coated with platinum. Pt-NPGL leaf membrane MEAs show good performance in our initial assessment here, showing a maximum power generated of ∼0.25 W cm^{-2} at Pt loads of ∼0.03 mg cm^{-2}, in our unoptimized test cell. Challenges remain in bringing this material to the mainstream, including optimization of testing conditions, examination of materials degradation (if any) over long period use, and replacement of the nanoporous gold supports with less expensive materials. However, generally, the strategy of making catalyst skins over nanoporous metal supports may be attractive as a means to reduce precious metal loading, eliminate the carbon catalyst support, and engineer new catalysts that take advantage of the strain engineering possible in these bilayer composite materials.

Acknowledgement

We gratefully acknowledge support for this work by the US Department of Energy Office of Basic Energy Sciences under grant DE-FG02-05ER15727.

References

[1] E.S. Smotkin, R.R. D'laz-Morales, Annu. Rev. Mater. Res. 33 (2003) 557.
[2] L. Zhang, J. Zhang, D.P. Wilkinson, H. Wang, J. Power Sources 156 (2006) 171.
[3] E. Antolini, Mater. Chem. Phys. 78 (2003) 563.
[4] E. Casado-Rivera, D.J. Volpe, L. Alden, C. Lind, C. Downie, T. Vázquez-Alvarez, A.C.D. Angelo, F.J. DiSalvo, H.D. Abruña, J. Am. Chem. Soc. 126 (2004) 4043.
[5] E. Antolini, J. Mater. Sci. 38 (2003) 2995.
[6] K.H. Kangasniemi, D.A. Condit, T.D. Jarvi, J. Electrochem. Soc. 151 (2004) E125.
[7] R. O'Hayre, S.-J. Lee, S.-W. Cha, F.B. Prinz, J. Power Sources 109 (2002) 483.
[8] T.R. Ralph, M.P. Hogarth, Platinum Met. Rev. 46 (2002) 117.
[9] J. Erlebacher, M.J. Aziz, A. Karma, N. Dimitrov, K. Sieradzki, Nature 410 (2001) 450.
[10] Y. Ding, Y.J. Kim, J. Erlebacher, Adv. Mater. 16 (2004) 1897.
[11] Y. Ding, M. Chen, J. Erlebacher, J. Am. Chem. Soc. 126 (2004) 6876.

[12] P. Landon, P.J. Collier, A.J. Papworth, C.J. Kiely, G.J. Hutchings, Chem. Commun. 18 (2002) 2058.
[13] T. Kinumoto, M. Inaba, Y. Nakayama, K. Ogata, R. Umebayashi, A. Tasaka, Y. Iriyama, T. Abe, Z. Ogumi, J. Power Sources 158 (2006) 1222.
[14] K.R. Cooper, V. Ramani, J.M. Fenton, H. Russell Kunz, Experimental Methods and Data Analysis of Polymer Electrolyte Fuel Cells, Scribner Associates Inc., 2005.
[15] Y. Chen, J. Washburn, Phys. Rev. Lett. 77 (1996) 4046.
[16] Y. Ding, A. Mathur, M. Chen, J. Erlebacher, Ang. Chem. Int. Ed. 44 (2005) 4002.
[17] M.Ø. Pedersen, S. Helveg, A. Ruban, I. Stensgaard, E. Lægsgaard, J.K. Norskov, F. Besenbacher, Surf. Sci. 426 (1999) 395.
[18] J. Luo, P. Njoki, Y. Lin, D. Mott, L. Wang, C.J. Zhong, Langmuir 22 (2006) 2892.
[19] I. Fried, The Chemistry of Electrode Processes, Academic Press, London, NY, 1973.
[20] H.A. Gasteiger, J.E. Panels, S.G. Yan, J. Power Sources 127 (2004) 162.
[21] J. Larminie, A. Dicks, Fuel Cell Systems Explained, second ed., John Wiley & Sons, Ltd., Hoboken, NJ, 2003.